약학석사학위논문

Therapeutic Effects of Chemical Inhibitors of AIMP2-DX2 and K-Ras Interaction on Lung Cancer

AIMP2-DX2와 K-Ras 단백질 간 결합 저해 물질의 폐암 치료 효과

2018년 2월

서울대학교 융합과학기술대학원
분자의학 및 바이오제약학과 의약생명과학전공

안 혜 원

Therapeutic Effects of Chemical Inhibitors of AIMP2-DX2 and K-Ras Interaction on Lung Cancer

AIMP2-DX2와 **K-Ras** 단백질 간 결합 저해 물질의
폐암 치료 효과

지도교수 김성훈

이 논문을 약학석사학위논문으로 제출함

2018 년 **2** 월

서울대학교 융합과학기술대학원
분자의학 및 바이오제약학과 의약생명과학전공
안 혜 원

안혜원의 석사학위논문을 인준함
2018 년 **2** 월

위 원 장 _____ (인)
부 위 원 장 _____ (인)
위 원 _____ (인)

ABSTRACT

Therapeutic Effects of Chemical Inhibitors of AIMP2-DX2 and K-Ras Interaction on Lung Cancer

Hyewon Ahn

Dept. of Molecular medicine and Biopharmaceutical Sciences

Graduate School of Convergence Science and Technology

Seoul National University

Aminoacyl-tRNA synthetase-interacting multifunctional protein 2 (AIMP2-F) is a tumor suppressor which interacts with several factors regulating cell death and growth arrest. In contrast, AIMP2-DX2, a splicing variant missing exon 2 of AIMP2-F, enhances tumorigenesis in human lung or colorectal cancer through competitive inhibitory function of AIMP2-F.

KRAS is proto-oncogene for making a protein called K-Ras protein that is involved in controlling cell division. When mutated, proto-oncogenes have the potential to cause normal cells to become cancerous. Especially, increase of mutated forms of K-Ras has been found in lung cancer patients. In previous study, AIMP2-DX2, an oncogenic variant of AIMP2, stabilizes K-Ras, and interaction of AIMP2-DX2 with K-Ras induced tumor growth. Therefore, we found therapeutic potential of interaction of AIMP2-DX2 with K-Ras in lung cancer treatment.

Here we set up a cell-based Nano-luciferase binary technology (NanoBiT) to monitor the

protein-protein interaction (PPI) between AIMP2-DX2 and K-Ras rapidly on 96-well scale. A total of 10000 compounds were screened for inhibitory activity on AIMP2-DX2 and K-Ras interaction, and 5 novel small molecule compounds were validated by various phenotypic experiments. Among those compounds, BC-DXI-27330 showed considerable lung cancer inhibitory efficacy in *in vitro*, cellular, and animal models. Through this research, we identified that the interaction between AIMP2-K-Ras is therapeutic target for human lung cancer and suggested effective small molecule compound as lung cancer medicine.

Key Words AIMP2-DX2, K-Ras, lung cancer, protein-protein interaction, NanoBiT assay, high-throughput screening (HTS)

Student Number 2016-26011

CONTENTS

LIST OF FIGURES

ABBREVIATION LIST

AIMP2 : Aminoacyl tRNA Synthetase complex-interacting multifunctional Protein 2

NanoBiT : Nano-luciferase Binary technology

HTS : High-throughput screening

PPI : Protein-protein interaction

MTT : 3-(4,5-dimethylthiazol-2-yl)-2,5-diphenyltetrazolium bromide

INTRODUCTION

Over the past decades, lung cancer used to be the frequently occuring cancer in both genders and one of the highest cause of death resulting from cancer all over the world. In this reason, there is a growing need to research and development of lung cancer therapy.

Recently, prevention and treatment of lung cancer is ongoing in various research institutes throughout the world. Chemotherapy can help control the spread and growth of the cancer. However, it cures lung cancer only a few patients and current lung cancer therapy is dependent on cytotoxic drugs. So many researchers are seeking better drugs to treat lung cancer to satisfy medical unmet needs what for limitation of existing drugs (1).

Aminoacyl-tRNA synthetase-interacting multifunctional protein 2 (AIMP2-F) contains 4 exons and plays a role as a tumor suppressor which regulates cell growth and death. AIMP2 has anti-proliferative activity by increasing cell growth arrest by TGF-β signal, also mediates pro-apoptotic activity through the activation of p53 and TNF-α. Conversely, AIMP2-DX2, an exon 2 depleted splicing variant of AIMP2-F, enhances tumorigenesis in human lung cancer through competitive inhibitory function of AIMP2-F. The destruction in the equilibrium between splicing variants or abnormal alternative splicing variants can help forward pathological disorder. In recent study, the expression of AIMP2-DX2 was induced by carcinogen like benzopyrene, and this mutation increases AIMP2-DX2 level that is related to lung cancer progression. Also, suppression of AIMP2-DX2 reduced tumor progression, so AIMP2-DX2 has an oncogenic potential. Previous studies have shown that AIMP2-DX2 can be studied as a therapeutic target or biomarker related with human lung cancer (2-8).

KRAS is proto-oncogene for making a protein called K-Ras protein that is involved in controlling cell division. When mutated, proto-oncogenes have the potential to

cause normal cells to become cancerous. Especially, increase of mutated forms of K-Ras has been found in lung cancer patients. Approximately 25-30% of lung cancer patients have K-Ras mutations, so it is a common tumorigenic event in lung cancer. Also, the survival rate of patients with KRAS mutation in tumor was lower compared with other patients (9-13). Several gene mutations have been showed in various cancers and the mutation target therapies have been gradually approved by Food and Drug Administration (FDA).

According to previous study, the expression of AIMP2-DX2, an oncogenic variant of AIMP2, was showed a positive correlation with K-Ras. In addition, the interaction of AIMP2-DX2 and K-Ras was determined regardless of mutation, and it is important for tumorigenic property by regulating protein stability of K-Ras. Therefore, the inhibition of oncogenic interaction between AIMP2-DX2 and K-Ras was implicated as a promising therapeutic target for lung cancer treatment.

High-throughput screening (HTS) is a method that uses fast and large scale processing to identify biological or biochemical activities of lots of compounds quickly (14). We tested known bioactive or drug-like small molecule libraries for seeking lung cancer therapeutic compounds.

Here, we use to discuss strategies for discovery and characterization of small-molecule inhibitors of protein-protein interactions. Protein-protein interactions have a significant role in many biological processes, and there is a large class of targets for human therapeutics. Nano-luciferase Binary Technology (NanoBiT), the leading edge system of high-throughput screening, can be applied for intracellular detection of protein-protein interactions. This system is composed of split nano-luciferase, and these two small tags minimizes its influence on the interaction of target proteins. When expressed in cells for monitoring complementation, Large BiT (LgBiT ; 17.6kDa) and Small BiT (SmBiT ; 11 amino acids)

constructs at the terminal of each protein come close enough to generate stable luminescent signal. This method can be used to detect interaction dynamics of proteins of interest quickly because the fusion of LgBiT and SmBiT is reversible (15-18).

In this study, we tested small molecule libraries to discover anti-carcinogenic compounds by NanoBiT assay. Here, we suggested that AIMP2-DX2 and K-Ras interaction is crucial for oncogenic activity and the blockage of this process can be effective approach to suppress lung cancer.

MATERIALS AND METHODS

Cell Culture

Chinese Hamster Ovary (CHO) cells were cultured using Rosewell Park Memorial Institute (RPMI) 1640 Medium (with 25 mM HEPES, L-Glutamine, Cat. SH30255.01) with 10% Fetal Bovine Serum (FBS, Hyclone, Cat. SH30919.03) and 1% penicillin/streptomycin (Hyclone, Cat. SV30010) and kept in 5% CO_2 incubator at 37°C. Plasmids were transfected by turbofect transfection reagents (Invitrogen) according to the manufacturer's protocols. For chemical treatment, cells were incubated with DMSO-based compounds in serum-free medium for 4 hours at 37°C atmosphere.

Nano-luciferase Binary Technology (NanoBiT) assay

CHO-K1 cells (2×10^6) were seeded with RPMI media in 100cm^2 plates. On the second day, LgBiT-AIMP2-DX2 and SmBiT-K-Ras DNAs were transiently transfected to the cells with Turbofect transfection reagent for 24hours. After seeding cells (2.5×10^4) in 96-well plate, cells were incubated with Nano-Glo live cell substrate (Promega) and buffer (Promega) about 10 min and luminescence signal was measured using Glomax 96 microplate luminometer (Promega).

Cell viability assay

H460 and WI-26 cells (5×10^3) were seeded in 96-well plates and treated with DMSO-based compounds in serum-free medium for 48 hours. 10 μl of 3-(4,5-dimethylthiazol-2-yl)-2,5-diphenyltetrazolium bromide (MTT) solution (5 mg/ml, Amresco) was added to each well containing 100 μl medium and incubated for 1~2 hours at 37 °C. The precipitated formazan crystals were dissolved in 100 μl DMSO (Duchefa). Absorbance was measured at 560 nm by Glomax 96 microplate luminometer (Promega).

Immunoblotting

Cells were washed and lysed in lysis buffer (50mM Tris-HCl, 150mM NaCl, 0.5% Triton X-100, 5mM EDTA, 10% glycerol, protease inhibitors and phosphatase inhibitors, pH 7.4) for 30 min at 4°C. Cells were collected into Eppendorf tubes and spun down for 30 min at 13,200 rpm at 4°C. The supernatants were transferred to a new tube and protein concentration was quantified by Bradford assay (Biorad, Cat. 500-0006). Proteins were mixed with sample buffer and lysis buffer and boiled samples for 8 min at 100°C. After that, each sample with marker protein was loaded on SDS-page gels depending on the size of protein of interest and separated by electrophoresis. The gel was transferred onto polyvinylidenefluoride (PVDF) membrane (Milipore, Cat. IPVH 00010) at constant 55mA, 6V for 1 hr 30 min and blocked with 5% skim milk based on 1% TBS-T for 30 min at room temperature to prevent non-specific bindings. The primary antibody was applied to the membrane either during overnight at 4°C or 1~2 hours at room temperature with rotation. Blots were washed 3 times for 5 min with TBS-T buffer and incubated with the secondary antibody for 1 hour at room temperature. The membranes were

washed 3 times repeatedly, and ECL solution was applied to the blots to develop to an x-ray film.

In vivo efficacy test

We produced LSL-K-Ras-G12D mouse model to test lung cancer inhibitory effect. Then, we dissolve the powder form of lead compound, BC-DXI-27330, in AIMP2-DX2 inhibitor solution. For preparation compound solution, we added 1,500 μl of DMSO, 100 μl of Tween-80, 3,000 μl of PEG-400 and vortexed well. After that, we added around 1/3 of 5,400 μl 1X PBS in drop-by-drop manner and vortexed briefly (the solution will turn into white and get warm). We added another 1/3 of PBS in drop-by-drop manner and residual 1/3 of PBS in sequence and vortexed thoroughly (15% DMSO, 1% Tween-80, 30% PEG, 55% PBS, final stock concentration is 1 mg/ml). It was diluted to 0.2 mg/ml and injected 10 μl/g ; 2 mpk/mouse. Finally, we examined micro CT before and after treatment that conducts intraperitoneal injection for 2 weeks.

RESULTS

Optimization of AIMP2-DX2:K-Ras Nano-luciferase Binary Technology (NanoBiT) assay

According to previous research, K-Ras is critical for cause of colorectal cancer by interaction with AIMP2-DX2. Nano-luciferase Binary Technology (NanoBiT) assay is good tools to study the interaction of two proteins. We set up NanoBiT assay platform to screen a small molecule library (Fig. 1A). There are eight possible combinations of expression tag positions of each protein, so we tested all configurations to determine the optimal orientation for fusion. Among those pairs, the interaction of LgBiT-tagged N-terminus of AIMP2-DX2 and SmBiT-tagged N-terminus of K-Ras gave the brightest and stable signal. LgBiT-tagged AIMP2-DX2 and K-Ras constructs were checked for their background signal because LgBiT was responsible for luciferase-enzyme activity (Fig. 1B). In addition, we checked that AIMP2-DX2 combined with K-Ras at a same ratio (Fig. 1C).

Compatibility of NanoBiT assay for high-throughput screening (HTS)

There are some parameters needed to be considered for high-throughput screening. It has to be considered these three conditions. Low CV% indicates high precision and Z' factor above 0.5 used as a measure of good assay quality. A series of experiments and analysis to prove that NanoBiT assay is reliably selecting compounds having an inhibitory effect. DMSO concentrations within 0 to 1% was at a steady state, therefore, any concentration up to 1% DMSO can be applied to this assay (Fig. 2A). After that, each well was treated 0.1% DMSO

equally to confirm signal consistency of AIMP2-DX2 and K-Ras NanoBiT assay in 96-well format. We repeated 3 times, and it was showed consistent signal in each plate and average of CV was under 10% (Fig. 2B, C). Low-by-low, column-by-column, and plate-to-plate statistical effect size (Z-factor) were up to 0.5. Z-factor is widely used as a measure of assay quality, and its values between 0.5 and 1 are good for high-throughput context. In conclusion, this assay is compatible for high-throughput screening.

Pilot screening by AIMP2-DX2:K-Ras NanoBiT assay using FDA-approved library compounds

Before a main research, we progressed pilot screening to test FDA-approved compounds by using AIMP2-DX2:K-Ras NanoBiT assay (Fig. 3A). From this screening, we selected the most effective chemical compound to make use of positive compound. Additionally, we identified reproducibility of inhibitory effect of positive compound (Fig. 3B).

Identification of small molecule inhibitors which suppress the AIMP2-DX2:K-Ras interaction

The inhibitory distribution for AIMP2-DX2 and K-Ras interaction about 10,000 drug-like small molecules from KRICT or professors with a collaborative research project were examined biochemically by high-throughput screening using AIMP2-DX2:K-Ras NanoBiT assay. Compounds which showed more than 80% inhibition were represented as red dots. The primary screening concentration was 3μM and its hit ratio was about 1% (Fig. 4A). In

sequence, a non-related protein-protein interaction, SmBiT-PRKACA and LgBiT-PRKAR2A, used as the positive control of screening to identify real-hits. The binding affinity of PRKACA:PRKAR2A is similar to that of AIMP2-DX2:K-Ras (Fig. 4B). H460 cells and WI-26 cells are lung cancer and normal cell line, respectively. H460 and WI-26 cells were treated with real-hits selected for 48 hours to determine their cell viability (Fig. 4C). The end-point cell metabolic activities were evaluated by 3-(4,5-dimethylthiazol-2-yl)-2,5-diphenyltetrazolium bromide (MTT) assay. It measures the activity of mitochondrial reductase. The primary screening concentration was 5 μM, and this experiment was repeated three times. I selected some compounds which reduced viability of lung cancer cell but not of normal cell.

Validation of hit compounds by dose-response NanoBiT assay and cell viability assay

We checked the inhibitory effect of real-hit compounds in a dose-dependent manner. Among them, BC-DXI-09850 and BC-DXI-27330 showed the most selectivity for AIMP2-DX2 and K-Ras interaction in comparison with PRKACA:PRKAR2A interaction (Fig. 5A). IC_{50} value (the half maximal inhibitory concentration) was calculated in the range of 3.5 to 8 x 10^{-7} M (Fig. 5B). After that, we tested selectivity for AIMP2-DX2 using inducible lung cancer cells (Inducible AIMP2-DX2 cell line and inducible Empty Vector cell line) by cell viability assay. BC-DXI-27330 reduced viability of inducible AIMP2-DX2 cells but not that of inducible empty vector cells in a dose-dependent manner (Fig. 5C, D). Although inhibitory concentration of BC-DXI-09850 is lower than that of BC-DXI-27330, the former was not

showed selectivity for AIMP2-DX2. From this assay, BC-DXI-27330 was selected as the primary lead for further validation research.

Tumor suppressive efficacy of BC-DXI-27330 in K-Ras driven lung cancer model

We established LSL-K-Ras-G12D mouse model to identify lung cancer inhibitory effect. For preparation the compound solution (1 mg/ml), we dissolved the powder form of lead compound in 15% DMSO, 1% Tween-80, 30% PEG, 55% PBS. It was injected intraperitoneally 5 times a week, twice (2 mpk). After 2 weeks we assessed lung cancer progression using *in vivo* micro CT. Compared with the vehicle-treated group as control, BC-DXI-27330 suppressed lung cancer growth *in vivo* (Fig. 6A, B). In addition, we compared histopathological change of lung tissues. To see whether BC-DXI-27330 induced apoptosis in tumor areas in lung, we also monitored the activation of caspase-3, a marker of cell apoptosis. The number of activated caspase-3 increased after BC-DXI-27330 treatment in both male and female. Furthermore, the expression level of AIMP2-DX2 and K-Ras decreased after BC-DXI-27330 treatment (Fig. 6C, D). No weight loss observed during this experiment (Fig. 6E).

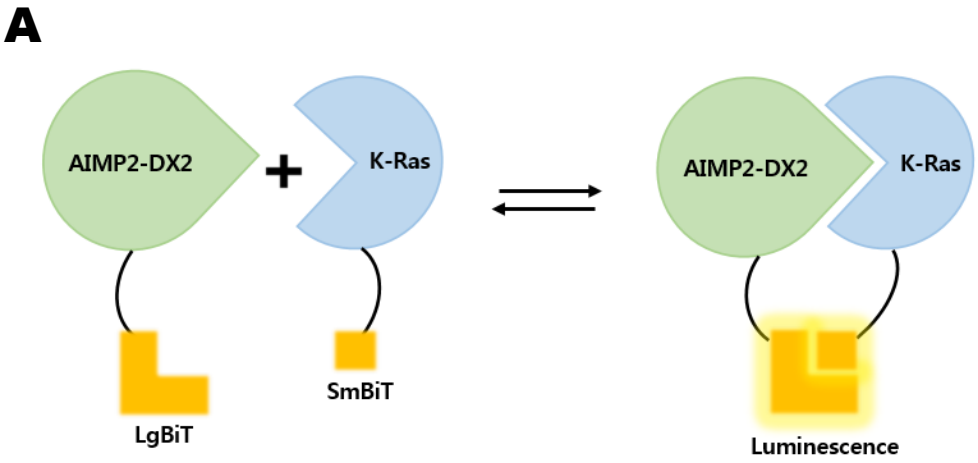
A
AIMP2-DX2
K-Ras
SmBiT
LgBiT
AIMP2-DX2
K-Ras
Luminescence

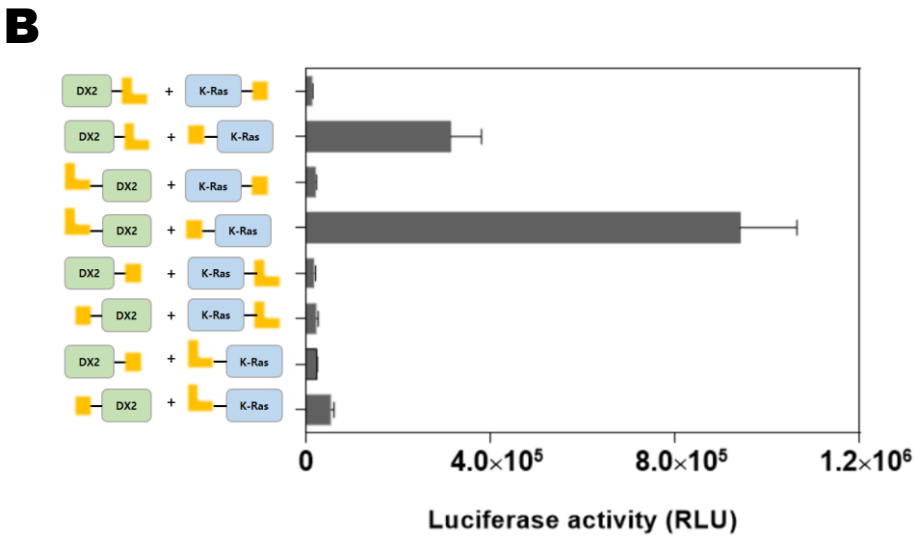
B
DX2
K-Ras
0
4.0×10⁵
8.0×10⁵
1.2×10⁶
Luciferase activity (RLU)

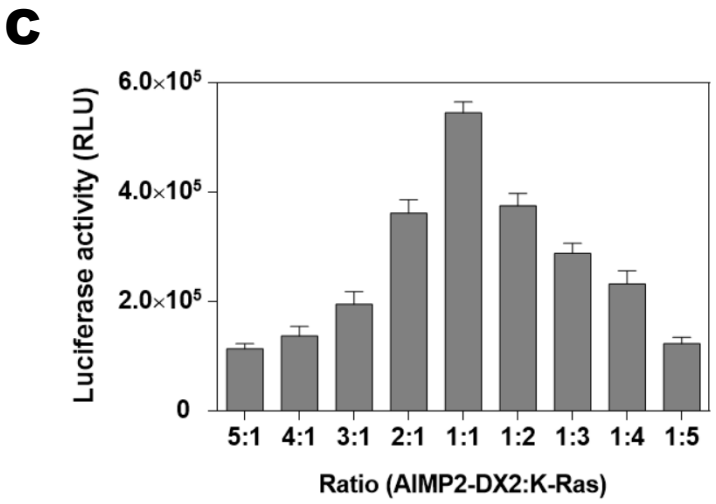
C
Luciferase activity (RLU)
6.0×10⁵
4.0×10⁵
2.0×10⁵
0
5:1
4:1
3:1
2:1
1:1
1:2
1:3
1:4
1:5
Ratio (AIMP2-DX2:K-Ras)

Figure 1. Optimization of AIMP2-DX2:K-Ras Nano-luciferase Binary Technology (NanoBiT) assay

(A) The schematic model of Nano-luciferase Binary Technology (NanoBiT) assay for AIMP2-DX2:K-Ras interaction.

(B) Eight possible combinations of luciferase tag positions. The pair of LgBiT-tagged N-terminus of AIMP2-DX2 and SmBiT-tagged N-terminus of K-Ras generated the most stable luminescence signal. LgBiT-tagged AIMP2-DX2 and K-Ras constructs were tested for their background signal because LgBiT was responsible for luciferase-enzyme activity.

(C) The stoichiometry of AIMP2-DX2:K-Ras interaction. AIMP2-DX2 combined with K-Ras at the ratio of 1:1.

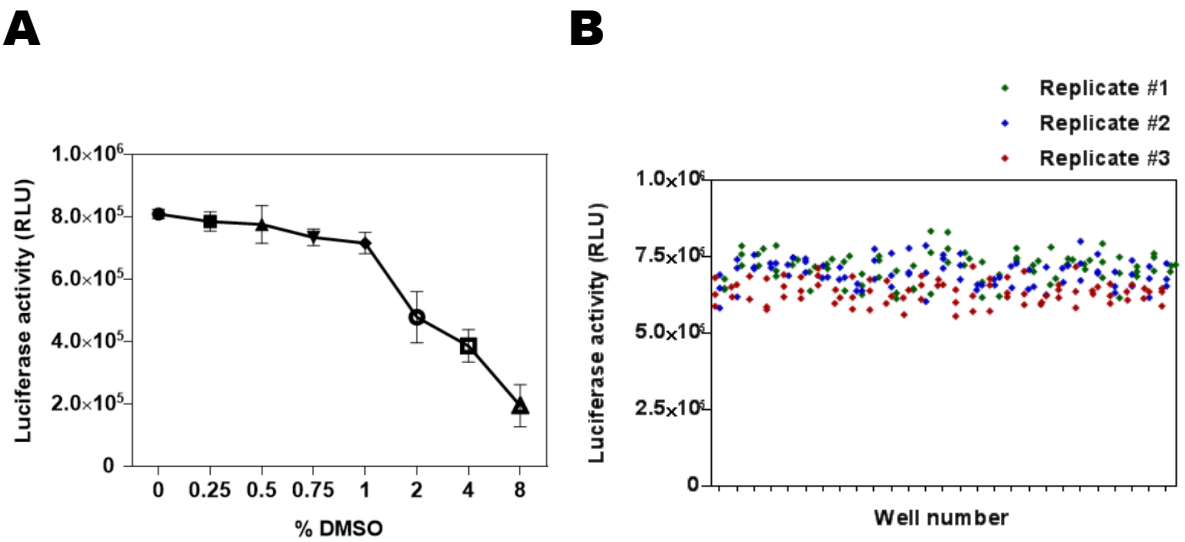

C

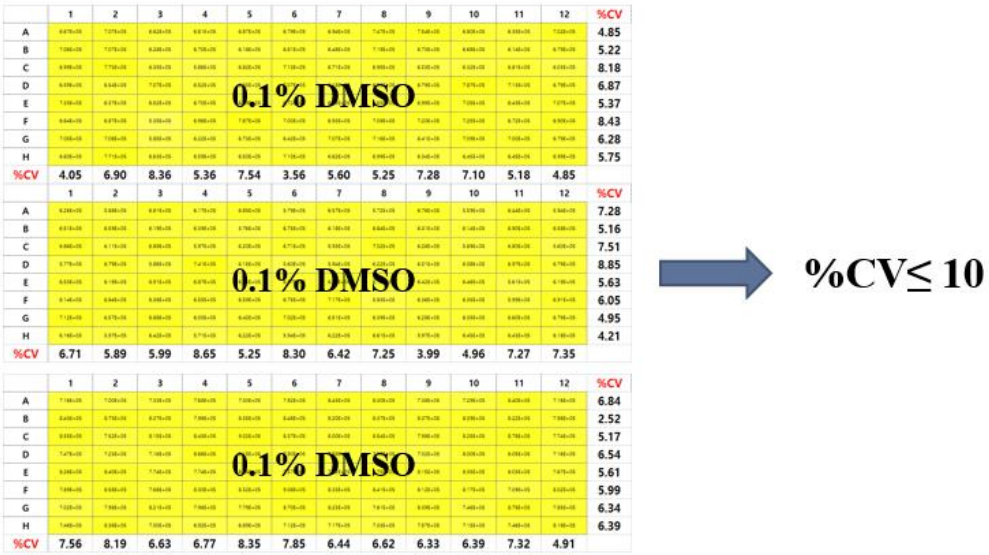

Figure 2. Compatibility of NanoBiT assay for high-throughput screening (HTS)

(A) DMSO tolerance test of AIMP2-DX2:K-Ras NanoBiT. 0~1% of DMSO concentrations was barely changed. Therefore, any concentration within this range can be applied to this assay. (B) and (C) Signal consistency of AIMP2-DX2:K-Ras NanoBiT assay in 96-well format. Each well was treated in 0.1% DMSO equally. We repeated 3 times, and it was showed consistent signal in each plate and average of CV was under 10%. Plate-to plate, column-by-column and low-by-low statistical effect size (Z-factor) were up to 0.5. Overall, it is compatible for high-throughput screening.

A

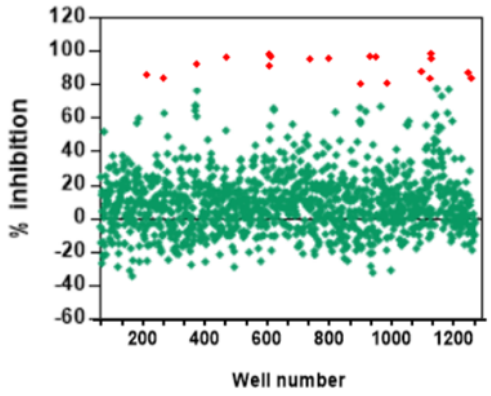

Total number of compounds	1,273
Concentration (μM)	5μM
Inhibition cutoff (%)	80 %
Number of hits	20
Hit ratio (%)	1.57%
Average Z' factor	0.65

B

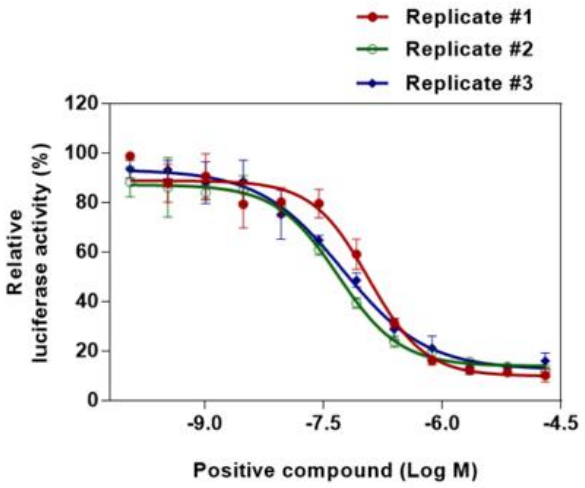

Figure 3. Pilot screening by AIMP2-DX2:K-Ras NanoBiT assay using FDA-approved library compounds

(A) Scatter plot distribution showing the results of the pilot screening using NanoBiT assay. The inhibition extent for AIMP2-DX2 and K-Ras interaction about 1,000 samples was examined by NanoBiT assay. Compounds which showed more than 80% inhibition were represented as red dots. The primary screening concentration was 5μM.

(B) Signal consistency of inhibitory effect of the most effective compound from this pilot screening. We utilized this compound as positive compound in high-throughput screening.

A

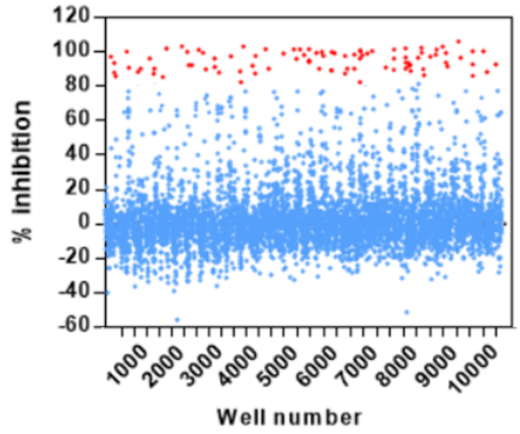

Total number of compounds	11,852
Concentration (μM)	5μM
Inhibition cutoff (%)	80 %
Number of hits	121
Hit ratio (%)	1.02%
Average Z' factor	0.82

B

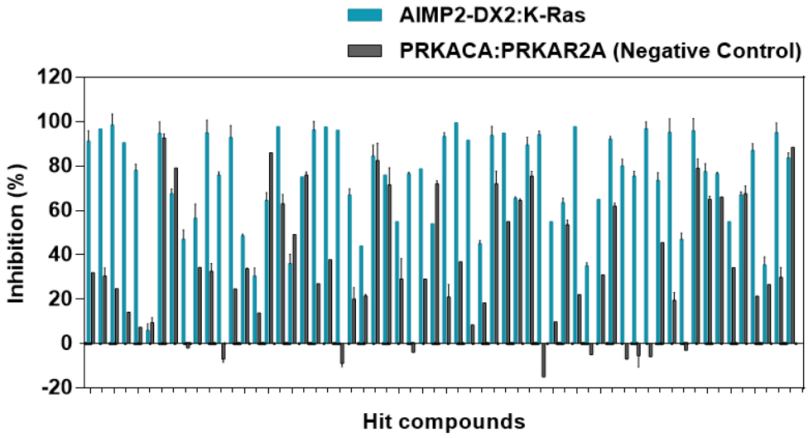

C

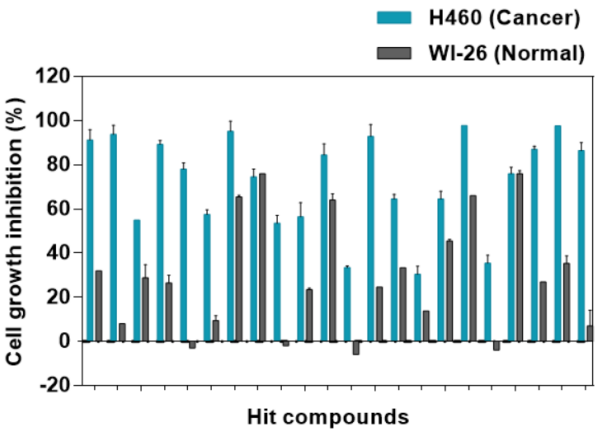

Figure 4. Identification of small molecule inhibitors which suppress the AIMP2-DX2:K-Ras interaction

(A) Scatter plot distribution showing the results of the high-throughput screening using AIMP2-DX2 and K-Ras NanoBiT assay. The inhibition extent of protein-protein interaction about 10,000 samples from KRICT or professors with a collaborative research project was examined by high-throughput screening. Compounds which showed more than 80% inhibition were represented as red dots. The primary screening concentration was 5 μM and its hit ratio was about 1%

(B) A non-related protein-protein interaction, SmBiT-PRKACA and LgBiT-PRKAR2A, was used as the positive control to identify real-hits. The binding affinity of PRKACA:PRKAR2A is similar to that of AIMP2-DX2:K-Ras.

(C) H460 and WI-26 cells were treated with real-hits for 48 hours to determine their cell viability. The end-point cell metabolic activities were evaluated by 3-(4,5-dimethylthiazol-2-yl)-2,5-diphenyltetrazolium bromide (MTT) assay. The primary screening concentration was 3 μM, repeated three times. H460 cells and WI-26 cells are lung cancer and normal cell line, respectively.

A

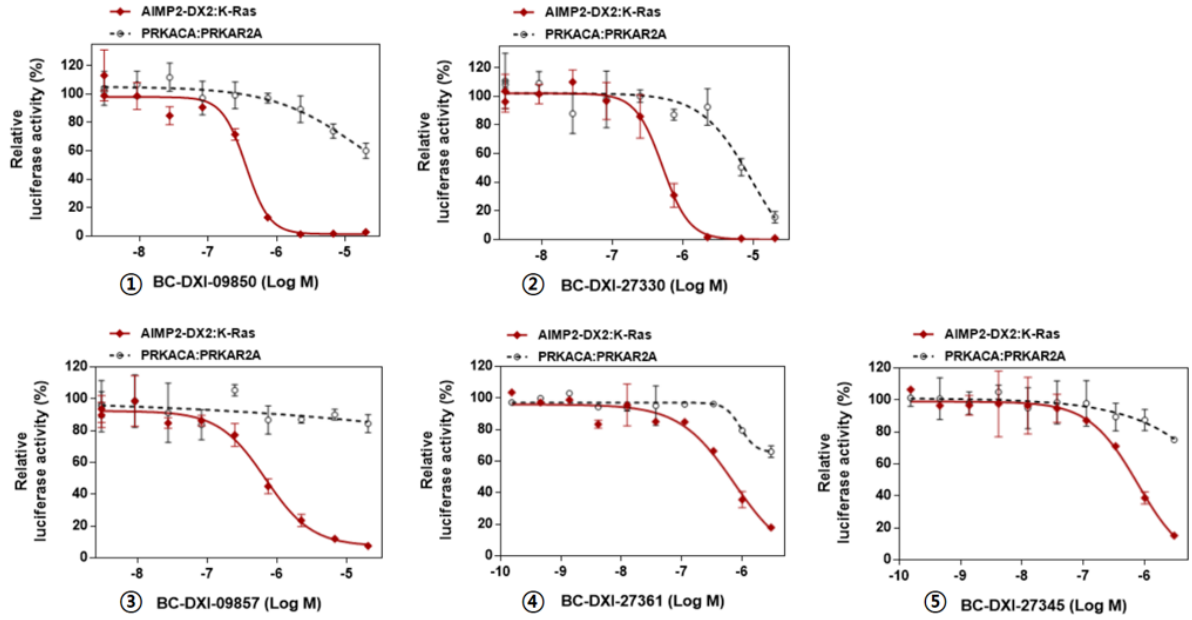

B

Compound	IC50(nM)
BC-DXI-09850	363.25±81.35
BC-DXI-27330	521.75±104.35
BC-DXI-09857	710.95±217.95
BC-DXI-27361	724.40±259.85
BC-DXI-27345	764.80±251.54

C

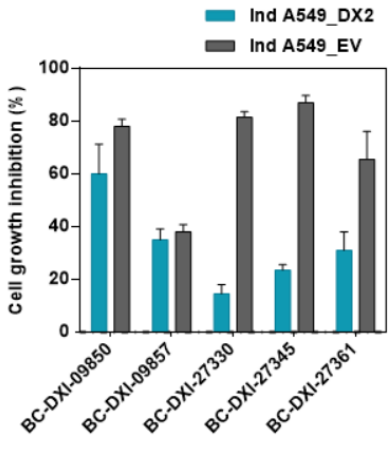

D

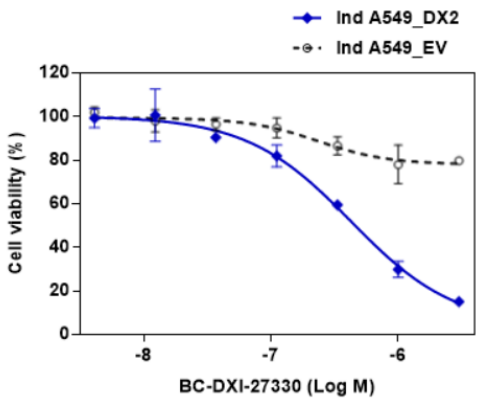

Figure 5. Validation of hit compounds by dose-response NanoBiT assay and cell viability assay

(A) The inhibitory effect of real-hit compounds in a dose-dependent manner (3-fold dilution). BC-DXI-09850 and BC-DXI-27330 showed the most selectivity for AIMP2-DX2 and K-Ras interaction in comparison with PRKACA:PRKAR2A interaction.

(B) IC_{50} value (the half maximal inhibitory concentration) was in the range of 3.5 to 8 x 10^{-7} M in NanoBiT assay.

(C) and (D) We checked selectivity for AIMP2-DX2 using inducible AIMP2-DX2 cancer cell line and inducible empty vector cancer cell line by cell viability assay. BC-DXI-27330 only reduced viability of inducible AIMP2-DX2 cells in a dose-dependent manner.

A

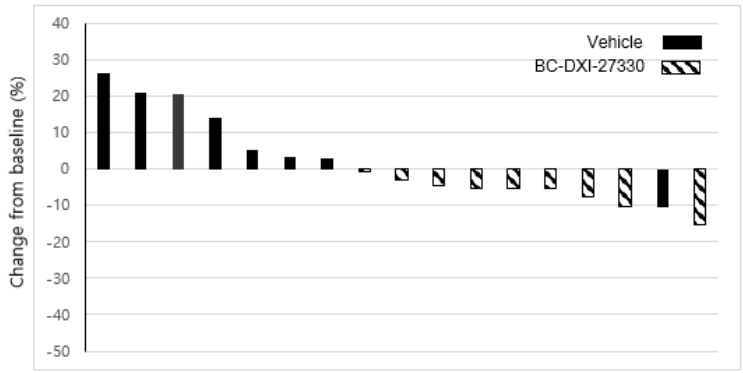

	Vehicle (N=8)	BC-DXI-27330 (N=9)	P value
Change	10.4 ± 12.3	-6.5 ± 4.2	0.005

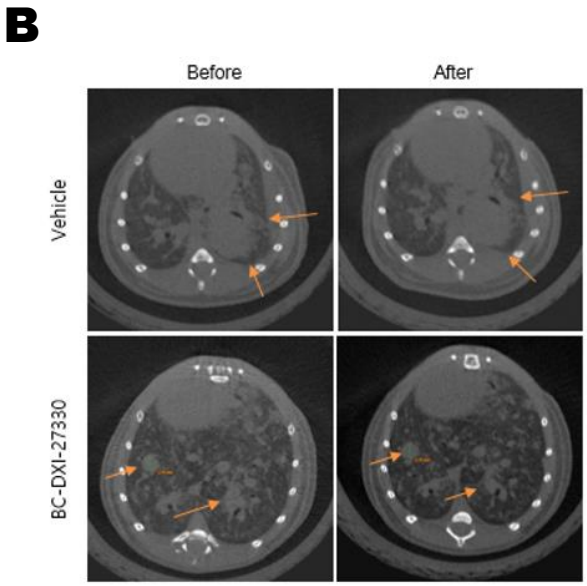
B
Before
After
Vehicle
BC-DXI-27330

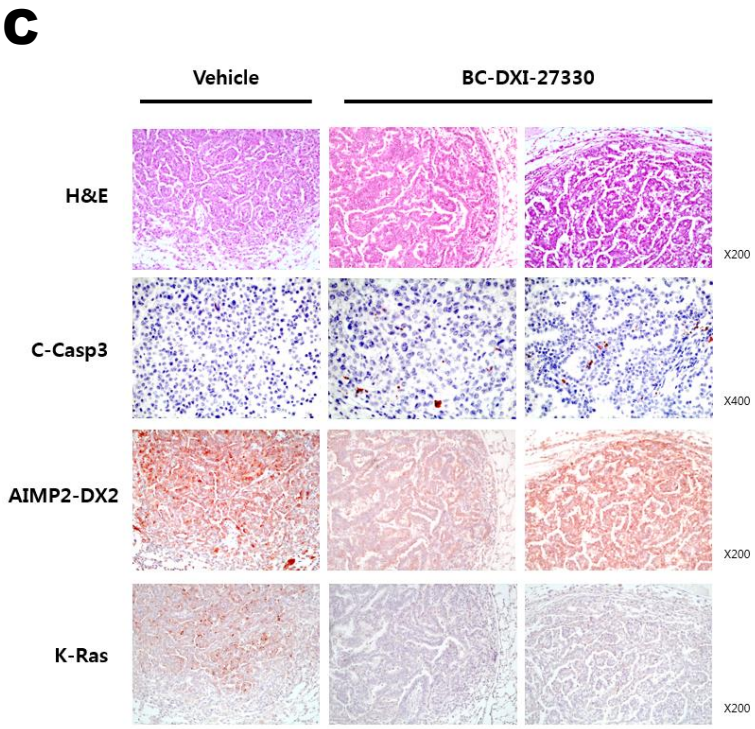
C
Vehicle
BC-DXI-27330
H&E
C-Casp3
AIMP2-DX2
K-Ras
X200
X400
X200
X200

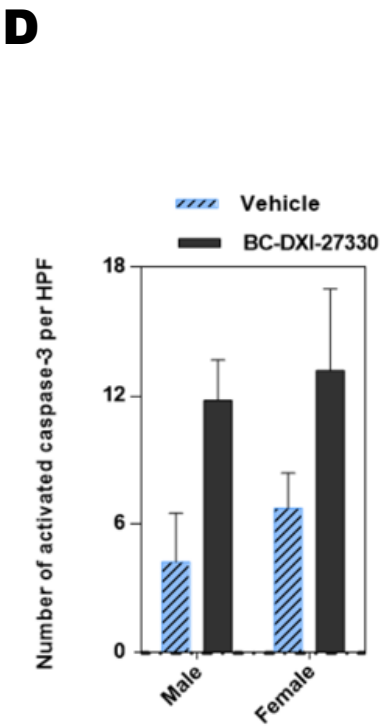
D
Vehicle
BC-DXI-27330
Number of activated caspase-3 per HPF
18
12
6
0
Male
Female

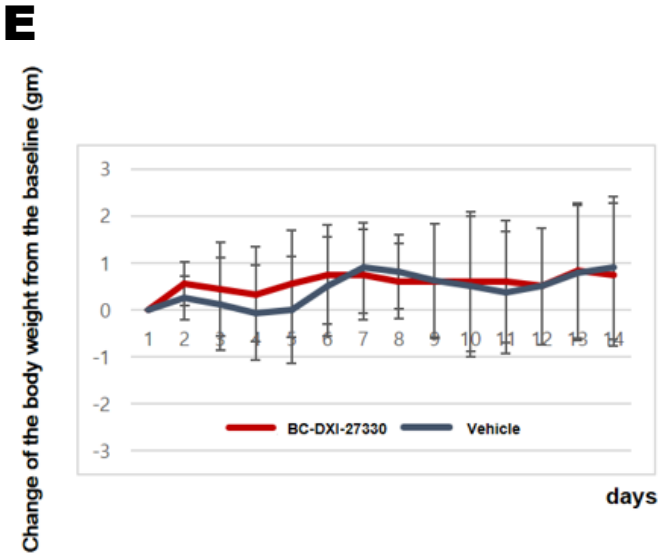

Figure 6. Tumor suppressive efficacy of BC-DXI-27330 in K-Ras driven lung cancer model

(A) and (B) The change and the representative images of inhibitory effect of lung cancer by micro CT in LSL-K-Ras-G12D mouse model. The compound (2 mpk) was intraperitoneally injected 10 times (5 times a week) for 2 weeks. BC-DXI-27330 suppressed lung carcinoma growth *in vivo*. BC-DXI-27330-treated lung tumors reduce more than vehicle-treated tumors.

(C) and (D) Histopathological comparison of lung tissues between the control and treated groups. Active caspase-3 positive parts are shown in red areas. The number of activated caspase-3 increased after BC-DXI-27330 treatment in both male and female. Also, the expression level of AIMP2-DX2 and K-Ras decreased after hit compound treatment.

(E) No weight loss observed during this experiment.

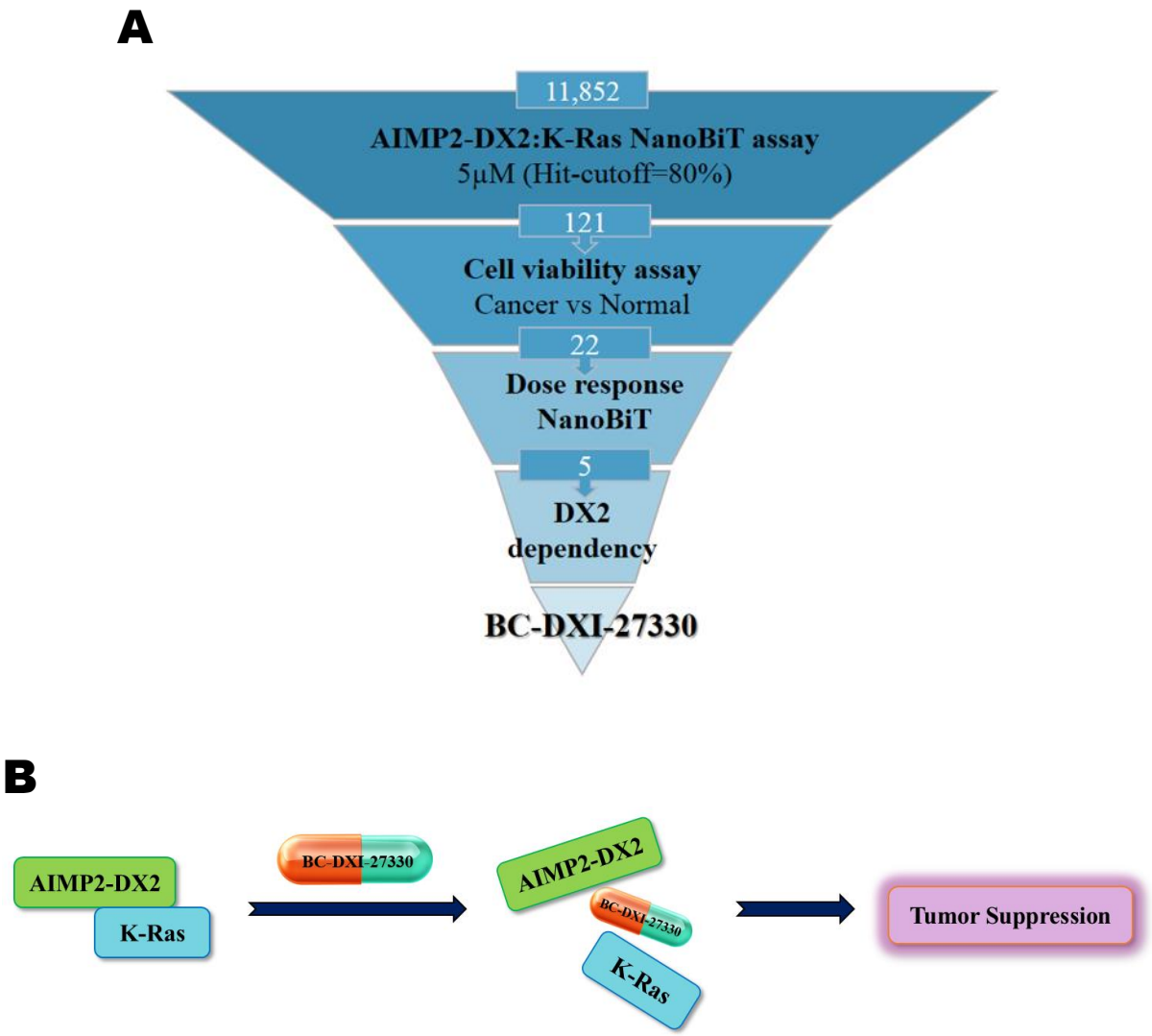

Figure 7. High-throughput screening workflow for AIMP2-DX2 and K-Ras interaction inhibitors

(A) Screening workflow of AIMP2-DX2 and K-Ras interaction inhibitors. BC-DXI-27330 was selectively inhibited AIMP2-DX2 and K-Ras interaction and suppressed lung cancer *in vitro* and *in vivo*.

(B) Schematic model of hit compound, BC-DXI-27330, which has high possibility to be a novel lung cancer drug.

DISCUSSION

Aminoacyl-tRNA synthetase-interacting multifunctional protein 2 (AIMP2-F) plays a role as a tumor suppressor and regulates cell growth and death in response to oncogenic signals. AIMP2-DX2 is an exon 2 alternative splicing variant of AIMP2-F, and its expression increased in cancer such as lung or colon cancer (5, 6). In this reason, AIMP2-DX2 can be studied as an effective therapeutic strategy to regulate cancer. In previous study, AIMP2-DX2 stabilizes K-Ras, and interaction of AIMP2-DX2 with K-Ras induces tumor growth. Therefore, AIMP2-DX2 and K-Ras interaction is crucial for oncogenic activity and the blockage of this process can be effective approach to suppress lung cancer.

In this research, we use to discuss strategies for discovery and characterization of small-molecule inhibitors of protein-protein interactions. Protein-protein interactions have an important role in many biological processes, and there is a large class of targets for human therapeutics (18). Nano-luciferase Binary Technology (NanoBiT), the cutting-edge strategy of high-throughput screening, can be used for intracellular detection of protein-protein interactions (15). NanoBiT use HSV-TK promoter to minimize possible non-specific background. We established this assay for high-throughput screening with reliable quality control.

We tested small molecule libraries to discover anti-carcinogenic compounds by NanoBiT assay. In this system, CHO cells were transfected with LgBiT-tagged N-terminus of AIMP2-DX2 and SmBiT-tagged N-terminus of K-Ras to express stable luminescence signal. A total of 10,000 compounds were screened for inhibitory activity on AIMP2-DX2 and K-Ras interaction, and 5 novel small molecule compounds were validated by various phenotypic experiments. We

performed MTT assay to sort hit compounds without cytotoxicity activity against WI-26 (normal lung cell line). BC-DXI-27330, the lead compound from protein-protein interaction based screening to target AIMP2-DX2 and K-Ras association, consistently reduced tumor progress in both human cancer cells and mouse models. The efficacy against cancer was dependent on the expression level of AIMP2-DX2 and K-Ras, but not to AIMP2. Also, we examined the decrease of lung cancer progression in LSL-K-Ras-G12D mouse model using *in vivo* micro CT imaging. The activation of caspase-3, a marker of apoptosis, is increased in lung carcinoma and the expression level of AIMP2-DX2 and K-Ras decreased after BC-DXI-27330 treatment.

In this research, we suggested that AIMP2-DX2 and K-Ras interaction is crucial for oncogenic activity and the inhibition of this process can be effective approach to suppress lung cancer. To summarize, we built up AIMP2-DX2 and K-Ras NanoBiT and performed this cell-based screening to select compounds that inhibit more than 80%. After that, we picked out some compounds that showed cancer-selectivity and dose-dependent inhibitory effect. Lastly, we found possible lead compound showed DX2-dependent inhibitory effect and confirmed tumor suppressive effect. Through this high-throughput screening strategy and target validation process, BC-DXI-27330, the lead compound from this study, will be the most therapeutic material targeting oncogenic interaction between AIMP2-DX2 and K-Ras. In conclusion, BC-DXI-27330 has high possibility to be a novel lung cancer drug that directly regulates the expression of an elusive target ‘K-Ras’ (9, 10).

REFERENCE

1. Cecilia Zappa and Shaker A. Mousa (2016) Non-small cell lung cancer: current treatment and future advances. Transl Lung Cancer Res. 5(3): 288–300. doi: 10.21037
2. Choi JW, Kim DG, Lee AE, Kim HR, Lee JY, *et al.* (2011) Cancer-Associated Splicing Variant of Tumor Suppressor AIMP2/p38: Pathological Implication in Tumorigenesis. PLOS Genetics 7(3): e1001351. doi: 10.1371/journal.pgen.1001351
3. Lee HS, Kim DG, Oh YS, Kwon NH, Lee JY *et al.* (2013) Chemical suppression of an oncogenic splicing variant of AIMP2 induces tumour regression. Biochem J. 454(3):411-6. doi: 10.1042/BJ20130550.
4. Park H, Park SG, Lee J-W, Kim T, Kim G, Ko Y-G, Kim S (2002) Monocyte Cell Adhesion Induced by a Human Aminoacyl-tRNA Synthetase Associated Factor, p43: Identification of the Related Adhesion Molecules and Signal Pathways. J Leukoc Biol 71: 223–230.
5. Choi JW, Um JY, Kundu JK, Surh YJ, Kim S (2009) Multidirectional tumor suppressive activity of AIMP2/p38 and the enhanced susceptibility of AIMP2 heterozygous mice to carcinogenesis. Carcinogenesis 30: 1638–1644.
6. Choi JW, Lee JW, Kim JK, Jeon HK, Choi JJ, *et al.* (2012) Splicing variant of AIMP2 as an effective target against chemoresistant ovarian cancer. J Mol Cell Biol. Jun;4(3):164-73. doi: 10.1093/jmcb/mjs018.

7. Sunghoon Kim, Sungyong You, and Daehee Hwang. (2011) Aminoacyl-tRNA synthetases and tumorigenesis : more than housekeeping. Nat. Rev. Cancer. doi: 10.1038/nrc3124
8. Park SG, Schimmel P, Kim S (2008) Aminoacyl tRNA synthetases and their connections to disease. Proc Natl Acad Sci U S A 105: 11043–11049.
9. Kempf E, Rousseau B, Besse B, Paz-Ares L (2015) KRAS oncogene in lung cancer: focus on molecularly driven clinical trials. Eur Respir Rev. 25(139):71-6. doi: 10.1183/16000617.0071.
10. Saveri Bhattacharya, Mark A. Socinski, and Timothy F. Burns (2015) *KRAS* mutant lung cancer: progress thus far on an elusive therapeutic target. Clin Transl Med. 2015; 4: 35. doi: 10.1186/s40169-015-0075-0
11. Wang Y, Kaiser CE, Frett B, Li HY. (2013) Targeting mutant KRAS for anticancer therapeutics: a review of novel small molecule modulators. J Med Chem. 11;56(13):5219-30. doi: 10.1021/jm3017706.
12. Kim HW, Park IK, Cho CS, Lee KH, Beck GR, Jr., et al. (2004) Aerosol delivery of glucosylated polyethylenimine/phosphatase and tensin homologue deleted on chromosome 10 complex suppresses Akt downstream pathways in the lung of K-ras null mice. Cancer Res 64: 7971–7976.
13. Matthew Patricelli MP, Janes MR, Li LS, Hansen R, Peters U *et al.* (2016) Selective Inhibition of Oncogenic KRAS Output with Small Molecules Targeting the Inactive State. Cancer Discov. 6(3):316-29. doi: 10.1158/2159-8290.
14. Paweł Szymański, Magdalena Markowicz, and Elżbieta Mikiciuk-Olasik (2012) Adaptation of High-Throughput Screening in Drug Discovery - Toxicological Screening Tests Int J Mol Sci. 13(1): 427–452. doi: 10.3390/ijms13010427

15. S Dixon, Andrew & Schwinn, Marie & P Hall, Mary & Zimmerman, Kris & Otto, *et al.* (2015) NanoLuc Complementation Reporter Optimized for Accurate Measurement of Protein Interactions in Cells. ACS chemical biology. doi: 10.1021/acschembio.5b00753
16. Jonathan Branch, Michael Quigley, Marco Gottardis and Ian Hickson (2016) A high-throughput PPI assay to quantify inhibition of androgen receptor variant 7 (AR-V7) binding to canonical AR full-length (AR-FL) binding partners. Cancer Research. doi: 10.1158/1538-7445
17. Paulmurugan, R. and Gambhir, S. S. (2007) Combinatorial library screening for developing an improved split-firefly luciferase fragment-assisted complementation system for studying protein-protein interactions. Anal. Chem. 79, 2346– 2353 doi: 10.1021/ac062053q
18. Michelle R. Arkin, Yinyan Tang, and James A. Wells (2014) Small-molecule inhibitors of protein-protein interactions progressing towards the reality. Chem Biol. 18; 21(9): 1102–1114. doi:10.1016/j.chembiol.

요약 (국문초록)

AIMP2-DX2와 K-Ras 단백질 간 결합 저해 물질의 폐암 치료 효과

안 혜 원 (Hyewon Ahn)

AIMP2-F (Aminoacyl-tRNA Synthetase-interacting multifunctional protein 2)는 세포의 성장과 사멸을 조절하는 여러 인자들과 상호작용 하면서 종양 형성 억제제로 작용하는 단백질이다. 반면 AIMP2-F를 이루고 있는 엑손 2가 결손된 splicing 변이체인 AIMP2-DX2는 AIMP2-F의 암 억제 기능을 방해하기 때문에 인간의 암, 특히 폐암이나 대장암의 발생을 증진시킨다.

KRAS는 세포의 분열을 조절하는 K-Ras라 불리는 단백질로 발현시키는 원발암 유전자 (proto-oncogene)이다. KRAS와 같은 원발암 유전자에 변이가 발생하면, 정상세포는 악성으로 진행할 가능성이 있다. 특히, K-Ras의 돌연변이는 폐암 환자에서 높게 발견할 수 있다. 이전 연구에 따르면 AIMP2-F의 종양 발생 변이체인 AIMP2-DX2가 K-Ras를 안정화시키며, AIMP2-DX2와 K-Ras 단백질 간의 상호작용이 암의 성장을 유발한다. 따라서, AIMP2-DX2와 K-Ras의 상호 결합 작용이 폐암 치료에 중요한 치료 전략이 될 수 있다.

본 연구는 AIMP2-DX2와 K-Ras의 단백질 간 결합 (PPI)을 96 well 플레이트에서 빠르게 측정할 수 있는 세포 기반 Nano-luciferase binary technology (NanoBiT)을 셋업하였다. 총 약 10000개 가량의 화합물들을 AIMP2-DX2와 K-Ras의 상호작용

저해 효과를 평가하였고, 5가지의 저분자 화합물을 추려 다양한 표현형을 확인하는 실험을 진행하였다. 이 중 BC-DXI-27330은 in vitro상에서, 세포 내에서, 동물 모델 모두에서 상당한 저해 효과가 있음을 알 수 있었다. BC-DXI-27330 화합물의 K-Ras의 발현을 직접적으로 조절할 수 있는 폐암 치료제로서의 가능성을 확인할 수 있었다. 결과적으로, 본 연구를 통해 AIMP2-DX2와 K-Ras 단백질 간 상호작용이 폐암 치료를 가능하게 할 수 있는 표적인자임을 확인하고, High-throughput screening (HTS)을 통해 폐암 억제 효과를 보이는 유효 물질을 제시하였다.

주요어 : AIMP2-DX2, K-Ras, 폐암, 단백질-단백질 상호작용, NanoBiT assay, 고속 대량 스크리닝 (HTS)

학 번 : 2016-26011